Letters

A Single-Layer UWB Frequency-Selective Surface With Band-Stop Response

Sayi Soundariya Sampath and Ramprabhu Sivasamy

***Abstract*—A single-layer compact frequency-selective surface (FSS) covering ultra-wideband application is presented in this letter. The proposed FSS constructed with convoluted elements exhibit band-stop response covering a frequency spectrum of 3.1–13.3 GHz at 10 dB. The prototype of the FSS is fabricated and the measured results seem to be in good agreement with the simulated result. Also, the designed FSS manifest polarization independent performance and good angular stability.**

***Index Terms*—Computer simulation technology (CST), frequency selective surfaces (FSS), transmit array, ultra-wideband (UWB).**

I. Introduction

FREQUENCY-selective surface (FSS) can be regarded as a periodic surface comprised of identical elements in a one-dimensional (1-D) or 2-D infinite array. 3-D FSSs with an additional degree of freedom in controlling its frequency response is also explored in the literature [1]–[5]. FSS have been most commonly used in dichroic reflectors, bandpass or band-stop filters, circuit analog absorbers, hybrid radomes, and microwave oven [6]. Wideband transmit array with reduced profile operating at 13.5 GHz consists of a pair of tri-layer FSS suitable for dual-polarization or circularly polarized applications [7]. The presented design maintains wide bandwidth and promising efficiency with its reduced profile by stacking multilayer FSS as the unit cell. The manual tuning device that uses bevel gears to control the spacing provides a large tuning range without the use of active devices [8]. Use of reconfigurable FSS for wideband shielding is on rise [9]. Broadband FSS with an embedded biasing network has been presented for electromagnetic (EM) shielding in different bands. The addition of varactor diodes shifts the band-stop response from higher to lower frequency. An ultra-wideband (UWB) FSS composed of hexagonal rings provide EM shielding for *S*- and *C*-band applications [10]. The 2.5-D hexagonal arrangement consists of metallic vias to connect the patches placed on the upper and lower layers. A broadband multilayer FSS uses active components to exhibit switching between two frequency bands [11]. The layers are stacked through air spacers, which accounts to multilayer geometry. Resistor-loaded FSS can be tuned to accomplish low-frequency and broadband absorption [12]. A single-layer FSS provides EM shielding for both *X*- and *Ka*-bands [13]. The coupling between the two printed elements of the FSS unit cell exhibits band-stop response. Compact UWB FSS has been designed by modifying the conventional loop type FSS [14]. The two metallic layers separated by a dielectric layer achieve wider bandwidth and higher order response. A compact UWB FSS with band-stop response is hitherto unexplored.

In this letter, the mutual coupling between parallel patches printed on the opposite surfaces of the substrate provides UWB response extended at its higher frequency range. The two layers of metallic unit cells on either side of the substrate achieve better miniaturization characteristic. This miniaturized periodic unit cell shows great stability with respect to incident angles and polarization. Section II describes the design principle of the FSS structure and its parametric details. The parametric sweep of the designed FSS is also elaborated. The analysis of the transmission characteristics of the evolved FSS unit cell is discussed in Section III. Prototype fabrication of the proposed FSS and experimental validation along with the measurement setup is explained in Section IV.

II. FSS Unit Cell Design

The unit cell design of the proposed FSS is composed of two metallic layers printed on both sides of the FR-4 substrate of thickness 1.6 mm, relative permittivity 4.3, and loss tangent 0.025. The metallic patch on the top is separated from the conducting ground plane by a dielectric material. The length, breadth, and height of the overall FSS are oriented along *x*-, *y*-, and *z*-axis, respectively. Classic Powell optimization method in computer simulation technology (CST) Microwave Studio Software [17] is used to obtain the final parameters of the proposed FSS. The final parameters of the FSS unit cell depicted in Fig. 1(a) and (b) are optimized as follows: $w = 0.3$ mm, $w1 = 0.45$ mm, $w2 = 0.15$ mm, $L1 = 1.46$ mm, $L2 = 2.07$ mm, and $P = 10$ mm. As the main objective of the proposed UWB FSS is to achieve miniaturization, 0.3 mm is chosen as the width of the proposed FSS geometry. The reason is twofold: the increase in

Manuscript received October 23, 2018; revised November 20, 2018; accepted November 28, 2018. Date of publication December 24, 2018; date of current version February 13, 2020. *(Corresponding author: Sayi Soundariya Sampath.)*

The authors are with the Department of Electronics and Communication Engineering, Sri Sivasubramaniya Nadar College of Engineering, Chennai 603110, India (e-mail: sayisoundariya@gmail.com; ramprabhus@ssn.edu.in).

Color versions of one or more of the figures in this letter are available online at http://ieeexplore.ieee.org.

Digital Object Identifier 10.1109/TEMC.2018.2886285

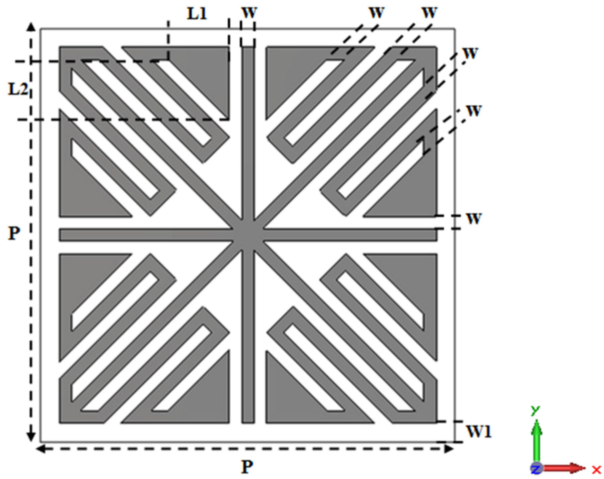

(a)

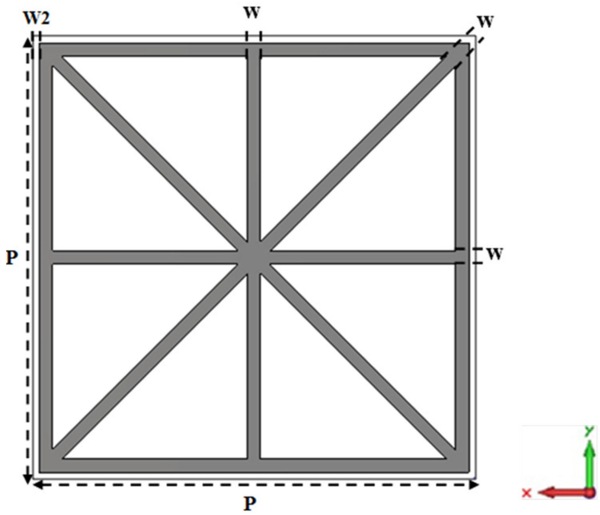

(b)

Fig. 1. (a) Top layer geometry of the proposed FSS unit cell with dimensions $w = 0.3$ mm, $w1 = 0.45$ mm, $L1 = 1.46$ mm, $L2 = 2.07$ mm, and $P = 10$ mm. (b) Bottom layer geometry of the proposed FSS unit cell with dimensions $w = 0.3$ mm, $w2 = 0.15$ mm, and $P = 10$ mm.

the width of the resonating arm beyond 0.3 mm restricts its usage in space constraint applications and decrease in the width of the resonating arm below 0.3 mm leads to fabrication difficulties.

The simulation results with passband and stopband characteristics are depicted in Fig. 2. It is evident from the transmission characteristics that the proposed FSS provides a band-stop response from 3.1 to 13.3 GHz at 10 dB reference level. Also, the reflection characteristics confirm the bandpass behavior of the proposed FSS. The design process begins with the design of unit cell elements in various levels. Its corresponding transmission characteristics are clearly depicted in Fig. 3. The resonant frequency of Level 1 structure starts from 4.5 GHz exhibiting broadband response. In Level 2 increase in the overall perimeter of the structure decreases the lowest frequency to 3.9 GHz. Further increase in the electrical length in Level 3 decreases the resonance to 3.1 GHz and hence providing UWB response.

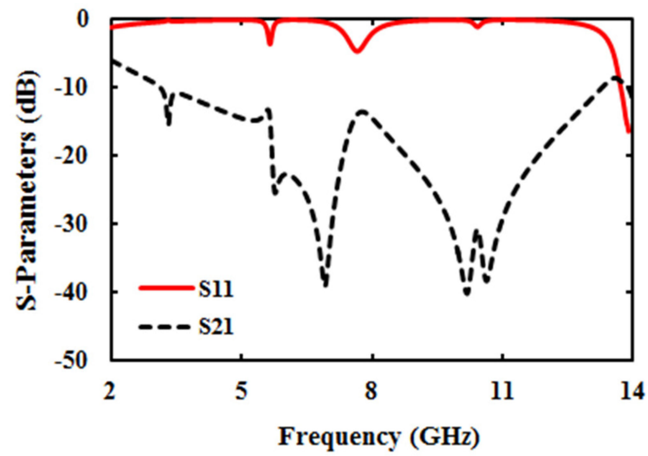

Fig. 2. *S*-parameter characteristics of the FSS.

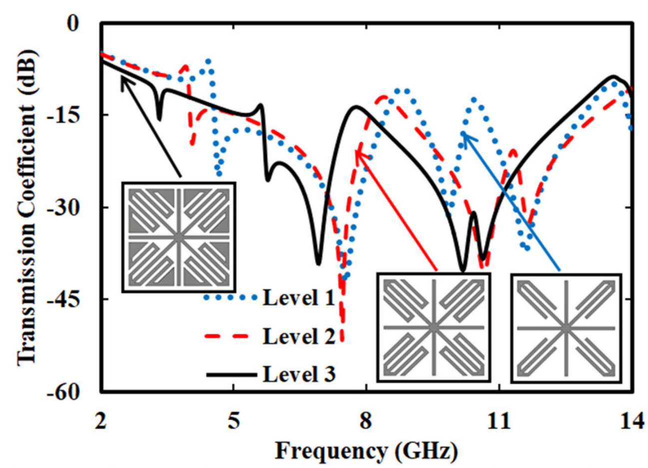

Fig. 3. Transmission characteristics of the proposed FSS in various levels.

III. Results and Analysis

The simulation software CST Microwave Studio [8] uses Floquet mode implementation with periodic boundary conditions. The transmission characteristics of the FSS with top, bottom, and a combination of both surfaces are illustrated in Fig. 4. The top layer of the FSS exhibits multi-band response at 3.6, 5.7, 9.7, and 10.7 GHz, whereas the bottom layer resonates at 7.4 GHz. It is observed that the configuration that combines top and bottom surfaces provides wide stopband characteristics and is attributed to the mutual coupling between its layers [13].

Surface current distribution at 10.18 and 6.92 GHz are depicted in Figs. 5 and 6, respectively. It is observed that the shorter arm with a small electrical length contributes to the higher resonance and the increased electrical length contributes to the lower resonance.

IV. Fabrication and Experimental Validation

A prototype of each of the top and bottom metallic layers consisting of 30 × 30 unit cells is fabricated on an FR4 substrate of thickness 1.6 mm. The overall dimension of the printed

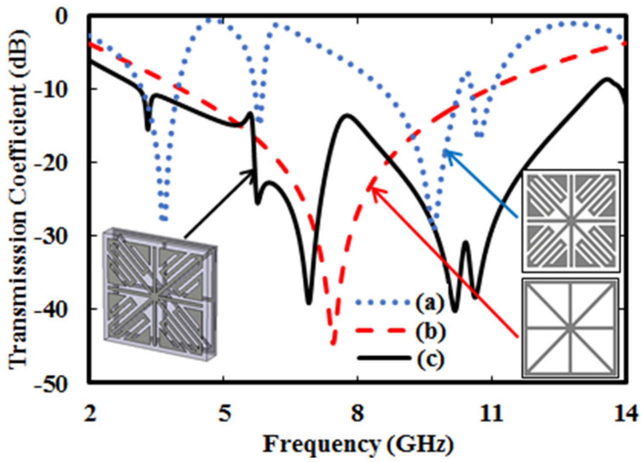

Fig. 4. Transmission characteristics. (a) Top layer. (b) Bottom layer. (c) Proposed FSS.

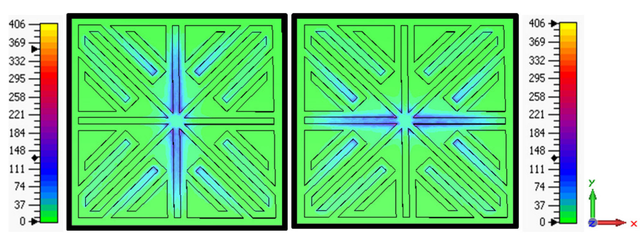

Fig. 5. Surface current distribution at 10.18 GHz

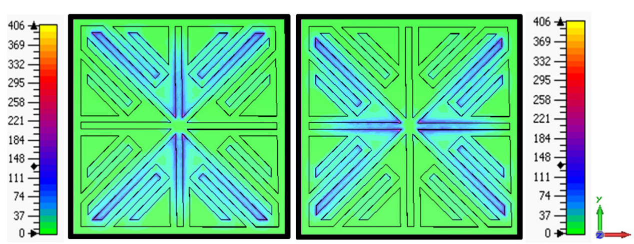

Fig. 6. Surface current distribution at 6.92 GHz

circuit board is 300 mm × 300 mm. The standard measurement setup illustrated in [14] is used to measure the performance of the fabricated FSS. The experiment has been carried out in a semi-anechoic chamber. Two pairs of horn antenna used in the measurements are JR-12 double-ridged horn antenna from Verdant Telemetry and KU5086 horn antenna from Vidyut Yantra Udyog. The horn antennas on either side of the FSS are about 1 m apart. Initially, the results are recorded without FSS, and then the fabricated prototype is placed between the transmitting and receiving antennas to perform the measurements. The measured transmission characteristics with and without FSS is depicted in Fig. 7. Comparison of the simulation and the measured transmission characteristics for transverse electric (TE) and transverse magnetic (TM) polarization of the proposed FSS are depicted in Figs. 8 and 9, respectively. It is apparent that the proposed FSS exhibits identical response for both polarization and stable for incident EM waves up to 45°. This satisfies the criteria of polarization independency and angular stability.

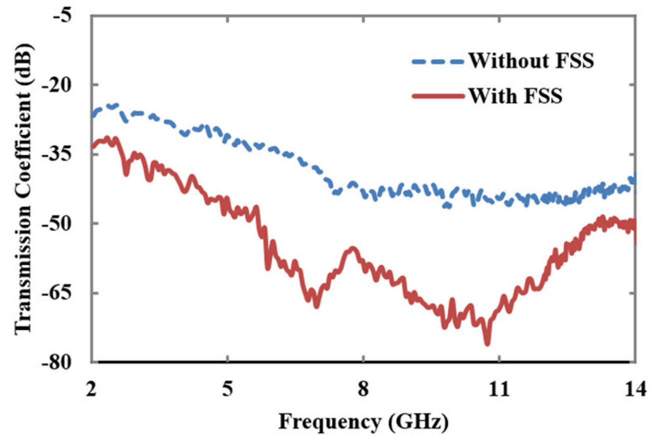

Fig. 7. Measured transmission characteristics with and without FSS.

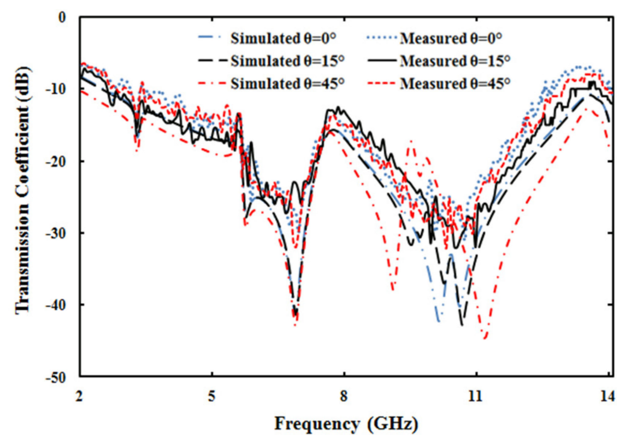

Fig. 8. Simulated and measured results of the FSS at oblique incidence for TE polarization.

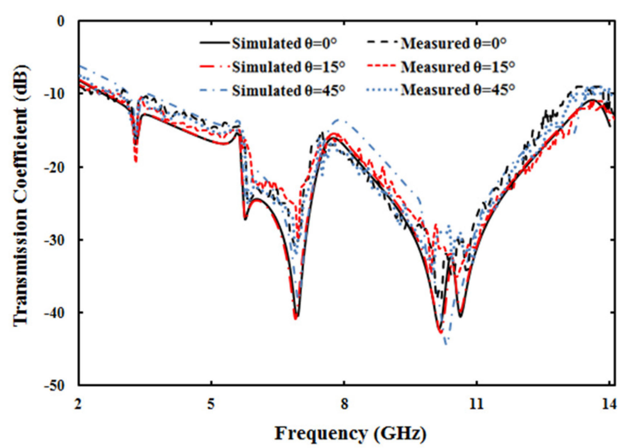

Fig. 9. Simulated and measured results of TM polarization at oblique incidence.

Table I compares the proposed work with the existing FSSs. The proposed FSS shows an improved bandwidth with miniaturized unit cell structure. The single-layer FSS exhibits an UWB frequency response.

TABLE 1
COMPARISON WITH THE EXISTING FSSS

Ref.	Unit cell size (mm)	Frequency range (GHz) at 10dB	Structure analysis	Angular Stability
[10]	11.1 x 9.6	1.97-8.08	2.5D MHRs with n-number of metallic vias to connect the metallic patches together.	Stable response upto 30°
[11]	11 x 11	3.18-12.78	Multilayer geometry with active p-i-n diodes.	Stable response upto 45°
[15]	20 x 20	8.2-12.4	Single and double-layer Sierpinski gasket fractal coated with composite materials.	Not reported
[16]	9 x 9	4.5-9.0	Parallel plate 3D FSS element with bandpass response.	Not reported
Proposed work	**10 x 10**	**3.1-13.3**	**A single layer UWB FSS with simple structure.**	**Stable operation upto 45°**

V. CONCLUSION

An UWB FSS with wide band-stop characteristics constructed with convoluted elements is presented in this letter. The proposed band-stop FSS with a compact structure exhibits a bandwidth of 10.2 GHz (3.1–13.3 GHz) at 10 dB reference level of insertion loss. The FSS provides good angular stability up to 45° and identical frequency response for both TE and TM polarization. The prototype of the FSS is fabricated and its simulated results are validated using measurements.

REFERENCES

[1] S. N. Azemi, K. Ghorbani, and W. S. T. Rowe, "3D frequency selective surface with incident angle independence," in *Proc. Eur. Microw. Conf.*, Nuremberg, Germany, 2013, pp. 928–931.

[2] M. H. Nisanci *et al.*, "Experimental validation of a 3D FSS designed by periodic conductive fibers Part-1: Band-pass filter characteristic," *IEEE Trans. Electromagn. Compat.*, vol. 59, no. 6, pp. 1841–1847, Dec. 2017.

[3] M. H. Nisanci *et al.*, "Experimental validation of a 3D FSS designed by periodic conductive fibers Part-2: Band-stop filter characteristic," *IEEE Trans. Electromagn. Compat.*, vol. 59, no. 6, pp. 1835–1840, Dec. 2017.

[4] M. Bouslama, M. Traii, A. Gharsallah, and T. A. Denidni, "Reconfigurable dual-band 3D frequency selective surface unit-cell," in *Proc. IEEE Int. Symp. Antennas Propag. USNC/URSI Nat. Radio Sci. Meeting*, Vancouver, BC, Canada, 2015, pp. 1264–1265.

[5] M. H. Nisanci, A. Y. Tesneli, N. B. Tesneli, and E. Tek, "Parameter analysis of a novel single layer 3D band-pass FSS designed by combination of continuous and discontinuous conductive rods," in *Proc. Prog. Electromagn. Res. Symp.*, Shanghai, China, 2016, pp. 3329–3332.

[6] B. A. Munk, *Frequency Selective Surfaces: Theory and Design*. New York, NY, USA: Wiley, 2000.

[7] Q. Luo, S. Gao, M. Sobhy, and X. Yang, "Wideband transmitarray with reduced profile," *IEEE Antennas Wireless Propag. Lett.*, vol. 17, no. 3, pp. 450–453, Mar. 2018.

[8] R. Sivasamy, B. Moorthy, M. Kanagasabai, V. R. Samsingh, and M. G. N. Alsath, "A wideband frequency tunable FSS for electromagnetic shielding applications," *IEEE Trans. Electromagn. Compat.*, vol. 60, no. 1, pp. 280–283, Feb. 2018.

[9] S. Ghosh and K. V. Srivastava, "Broadband polarization-insensitive tunable frequency selective surface for wideband shielding," *IEEE Trans. Electromagn. Compat.*, vol. 60, no. 1, pp. 166–172, Feb. 2018.

[10] B. Hua, X. He, and Y. Yang, "Polarisation-independent UWB frequency selective surface based on 2.5D miniaturised hexagonal ring," *Electron. Lett.*, vol. 53, no. 23, pp. 1502–1504, Nov. 2017.

[11] S. Ghosh and K. V. Srivastava, "A polarization-independent broadband multilayer switchable absorber using active frequency selective surface," *IEEE Antennas Wireless Propag. Lett.*, vol. 16, pp. 3147–3150, 2017.

[12] J. Li *et al.*, "Design of a tunable low-frequency and broadband radar absorber based on active frequency selective surface," *IEEE Antennas Wireless Propag. Lett.*, vol. 15, pp. 774–777, 2016.

[13] I. S. Syed, Y. Ranga, L. Matekovits, K. P. Esselle, and S. Hay, "A single-layer frequency-selective surface for ultrawideband electromagnetic shielding," *IEEE Trans. Electromagn. Compat.*, vol. 56, no. 6, pp. 1404–1411, Dec. 2014.

[14] N. Kushwaha, R. Kumar, R. V. S. Ram Krishna, and T. Oli, "Design and analysis of new compact UWB frequency selective surface and its equivalent circuit," *Prog. Electromagn. Res. C*, vol. 46, pp. 31–39, 2014.

[15] C. Pelletti, G. Bianconi, R. Mittra, and Z. Shen, "Frequency selective surface with wideband quasi-elliptic bandpass response," *Electron. Lett.*, vol. 49, no. 17, pp. 1052–1053, Aug. 2013.

[16] R. Panwar, S. Puthucheri, V. Agarwala, and D. Singh, "Fractal frequency-selective surface embedded thin broadband microwave absorber coatings using heterogeneous composites," *IEEE Trans. Microw. Theory Techn.*, vol. 63, no. 8, pp. 2438–2448, Aug. 2015.

[17] [Online]. Available: https://www.cst.com/products/csts2/optimization/local-optimizer

Sayi Soundariya Sampath received the B.E. degree in electronics and communication engineering and the M.E. degree in communication systems. She is currently working toward the Ph.D. degree at the Department of Electronics and Communication Engineering, Sri Sivasubramaniya Nadar College of Engineering, Chennai, India.

She was a Research Assistant with the Department of Electronics and Communication Engineering, Sri Sivasubramaniya Nadar College of Engineering, in 2016. Her research interests include frequency selective surfaces, antenna design, and EMI/EMC.

Ramprabhu Sivasamy received the B.E. degree in electronics and communication engineering from Kongu Engineering College, Anna University, Chennai, India, and the M.E. and Ph.D. degrees from Anna University.

He is currently an Associate Professor with the Department of Electronics and Communication Engineering, Sri Sivasubramaniya Nadar College of Engineering, Chennai, India. His research interests include frequency selective surfaces, electromagnetic shielding, and microwave component design.